

Preferential Physical and Functional Interaction of Pregnane X Receptor with the SMRT α Isoform

Chia-Wei Li, Gia Khanh Dinh and J. Don Chen

Department of Pharmacology, University of Medicine and Dentistry of New Jersey, Robert
Wood Johnson Medical School, Piscataway, New Jersey

Running Title:

SMRT α Preferentially Regulates PXR Activity

Corresponding Author:

J. Don Chen, Ph.D. Department of Pharmacology, UMDNJ-Robert Wood Johnson Medical School, 661 Hoes Lane, Piscataway, New Jersey 08854-5635 USA. email: chenjd@umdnj.edu

Document Statistics:

Number of text pages: 36

Table: 0

Figures: 6

References: 40

Word counts: Abstract: 226; Introduction: 736; Discussion: 671

Abbreviations: PXR, pregnane X receptor; SMRT, silencing mediator for retinoid and thyroid hormone receptors; N-CoR, nuclear receptor corepressor; NR, nuclear receptors; HDAC, histone deacetylase; ID, interacting domain; RXR, retinoid X receptor; DR3, direct repeats spaced by 3 nucleotides; ER6, everted repeats separated by 6 nucleotides; MDR1, multidrug resistance 1; iNOS, nitric oxide synthase; CAR, constitutive androstane receptor; TR, thyroid hormone receptor; PCN, pregnenolone-16 α -carbonitrile; ONPG, o-nitrophenyl β -D-galactopyranoside.

ABSTRACT

The silencing mediator for retinoid and thyroid hormone receptors (SMRT) serves as a platform for transcriptional repression elicited by several steroid/nuclear receptors and transcription factors. SMRT exists in two major splicing isoforms: α and τ , with SMRT α contains only an extra 46-amino acid sequence inserted immediately downstream from the C-terminal corepressor motif. Currently little is known about potential functional differences between these two isoforms. Here we show that the pregnane X receptor (PXR) interacts more strongly with SMRT α than with SMRT τ both *in vitro* and *in vivo*. Interestingly, the PXR-SMRT α interaction is also resistant to PXR ligand-induced dissociation, in contrast to the PXR-SMRT τ interaction. Consistently, SMRT α inhibits PXR activity more efficiently than does SMRT τ in transfection assays, while they possess comparable intrinsic repression activity and association with histone deacetylase. We further show that the mechanism for the enhanced PXR-SMRT α interaction involves both the 46-amino acid insert and the C-terminal corepressor motif. Specifically, the first five amino acids of the SMRT α insert are essential and sufficient for the enhanced binding of SMRT α to PXR. Furthermore, we demonstrate that Tyr 2354 and Asp 2355 residues of the SMRT α insert are most critical for the enhanced interaction. Additionally, expression data show that SMRT α is more abundantly expressed in most human tissues and cancer cell lines, and together these data suggest that SMRT α may play a more important role than SMRT τ in the negative regulation of PXR.

INTRODUCTION

Transcriptional regulation is a dynamic process involving both association and dissociation of the transcription factor with various coactivators and corepressors. One well-investigated system is the prominent effects of coactivators and corepressors on the transcriptional activity of steroid/nuclear hormone receptors (NRs) (Westin et al., 2000). The silencing mediator of retinoid and thyroid hormone receptors (SMRT) (Chen and Evans, 1995b; Ordentlich et al., 1999; Park et al., 1999) and the nuclear receptor corepressor (N-CoR) (Horlein et al., 1995) are two related corepressors known to mediate repression by several unliganded NRs through recruitment of histone deacetylases (HDACs) (Guenther et al., 2000; Nagy et al., 1997). These corepressors are believed to act as protein platforms for the assembly of corepressor complexes necessary for transcriptional repression. Transcription repression is an important genomic event involved in many physiological processes such as development, homeostasis, cell growth, and differentiation (Privalsky, 2004).

In the absence of ligand, SMRT and N-CoR bind to the unliganded receptor through their NR-interacting domains (IDs) (Ghosh et al., 2002; Hu and Lazar, 1999). Upon ligand binding, the receptors undergo a conformational change, leading to alteration of the corepressor-binding pocket that causes release of corepressors and recruitment of coactivators. The human pregnane X receptor (PXR, also known as SXR and PAR) is a promiscuous sensor for several xenobiotic compounds (Watkins et al., 2001), and it binds to a diverse group of endogenous and exogenous ligands (Moore et al., 2003; Synold et al., 2001). Functionally, PXR directly activates a subset of genes involved in drug metabolism (Xu et al., 2002). Therefore, drugs that activate PXR are

likely to cause a higher risk of drug-drug interactions (Harmsen et al., 2007; Urquhart et al., 2007; Wipf et al., 2007).

The ability of PXR to regulate gene expression depends on its ability to form heterodimers with the retinoid X receptor (RXR) and bind to several PXR response elements. Several PXR response elements are found within the *CYP3A* promoters configured as direct repeats separated by 3 nucleotides (DR3) (Kliewer et al., 1998), everted repeats separated by 6 nucleotides (ER6) (Lehmann et al., 1998), or inverted repeats separated by 8 nucleotides (IR8) (Kast et al., 2002). In addition, the PXR-RXR heterodimers also bind tightly to several natural DR4 (direct repeats separated by 4 nucleotides)-type response elements. These include a DR4 motif in the intestinal multidrug resistance (*MDR1*) gene promoter responsible for its induction by rifampin (Geick et al., 2001) and a similar motif in the nitric oxide synthase (*iNOS*) promoter responsible for its induction by clotrimazole (Toell et al., 2002), both through the PXR-RXR heterodimers. Consistently, PXR-RXR heterodimers also bind well to synthetic AG(G/T)TCA repeats of different spacing with a preferred affinity toward a DR4 element (Blumberg et al., 1998). Once activated, the PXR-RXR heterodimer recruits transcriptional coactivators such as the p160 proteins (Leo and Chen, 2000) to form a multiprotein complex to activate transcription (Kliewer et al., 1998). In addition, PXR can also cross-talk with other NR response elements, including those recognized by the constitutive androstane receptor (CAR) (Kodama et al., 2004; Muangmoonchai et al., 2001), and the antioxidant response element on the rat glutathione *S*-transferase A2 gene (Falkner et al., 2001).

Currently, it is known that SMRT exists in cells at least as two major splicing isoforms: α and τ (Goodson et al., 2005). In comparison to SMRT τ , SMRT α contains an extra small exon encoding a 46-amino acid sequence inserted after residue G2352, immediately downstream to the distal corepressor motif (ID2, residues 2342-2350). SMRT α and SMRT τ reportedly interact with thyroid hormone receptors (TRs) with different affinities (Goodson et al., 2005); however, the molecular mechanism of such a differential affinity remains unknown. SMRT τ has also been shown to interact directly with and regulate the transcriptional activity of PXR in a PXR-ligand sensitive manner (Johnson et al., 2006; Wang et al., 2006); however, it was unknown if and how PXR might interact with SMRT α . In this study, we have compared the binding affinities between SMRT α and SMRT τ toward several NRs, with a focus on PXR. We found that, in contrast to other NRs, PXR uniquely displayed a preferential binding toward SMRT α . Intriguingly, this SMRT α interaction is resistant to PXR ligand-induced dissociation, and SMRT α elicited a greater inhibition on PXR activity than SMRT τ . Importantly, we also uncovered critical residues in SMRT α that are responsible for its higher affinity toward PXR, and showed that SMRT α is the dominant form expressed in most surveyed human tissues and cancer cells.

MATERIALS AND METHODS

Chemicals - Rifampicin (Rif), clotrimazole (CTZ), and pregnenolone-16 α -carbonitrile (PCN) were purchased from Sigma (St. Louis, MO). The rabbit anti-HA and mouse anti-FLAG antibodies were purchased from MBL and Stratagene, respectively. All other reagents, including culture media for bacteria, yeast and mammalian cells were purchased from standard sources.

Plasmids - The expression vectors pGEX-SMRT τ S1/2 (aa 2077-2471) and pGEX-SMRT α S1/2 (aa 2077-2517) were as previously described (Goodson et al., 2005) and kindly provided from Dr. Martin Privalsky. The pCMX-FLAG-cSMRT τ (2095-2471) and pCMX-FLAG-cSMRT α (2095-2517) were constructed by subcloning the Hind III to NheI fragments of pGEX-SMRT τ S1/2 and pGEX-SMRT α S1/2 into the pCMX-FLAG vector, respectively. The SMRT ID1 (aa 2107-2187), SMRT τ ID2 (aa 2284-2379), SMRT α ID2 (aa 2284-2425), SMRT τ ID1-2 (aa 2107-2379), and SMRT α ID1-2 (aa 2107-2425) fragments were generated by PCR reactions with *pfu* polymerase (NEB, Beverly, MA), and subcloned into various plasmid vectors. The full-length pCMX-F-SMRT τ and pCMX-F-SMRT α were constructed by assembling the Asp718 to Hind III fragment of pCMX-hSMRTe (Park et al., 1999) into the pCMX-FLAG-cSMRT τ and pCMX-FLAG-cSMRT α plasmids, and then subcloned into pEGFP-C1 and pCMX-GAL4 plasmids at Asp718 and NheI sites. The full-length human PXR (hPXR) and its Δ AF2 (aa 1-422) mutant in pGBT9, pCMXHA, and pCMX-GAL4 vectors were as previously described (Johnson et al., 2006). The point mutations mID1 (V2142A/I2143A), mID2 (I2345A/I2346A), mID1-2 (V2142A/I2143A, I2345A/I2346A), m3 (S2285E/K2286E/K2287E), and m4 (L2467A/I2468A, based on SMRT α sequence) were as previously described (Ghosh et al., 2002). These point mutants were regenerated in the SMRT α template by QuickChange site-directed mutagenesis (Stratagene, La Jolla, CA). All constructs were double confirmed by restriction enzyme digestion and DNA sequencing, and further information is available upon request.

Yeast Two-Hybrid Assay – The GAL4 DBD fusion constructs (in pGBT or pAS vector) were cotransformed in combination with GAL4 activation domain (AD) fusion constructs (in pACT or pGAD vector) into yeast Y190 cells as indicated in individual experiments. Transformed cells

were grown in synthetic complete media lacking tryptophan and leucine (-Trp -Leu) at 30 °C for 24 hours. Aliquots (100 μ l) from individual cultures were added to 3mL fresh selection medium, supplemented with solvent (DMSO) or indicated ligands. Cells were harvested 24 hours later and analyzed by liquid β -galactosidase assay using o-nitrophenyl β -D-galactopyranoside (ONPG) as substrate. The average β -galactosidase units were calculated from three separate colonies.

GST Pull-Down Assay - GST and GST fusion proteins were expressed in bacteria BL21 cells and purified by glutathione agarose beads by standard procedure. Individual nuclear receptors were synthesized and labeled with [³⁵S]-methionine in rabbit reticulocyte lysate via TNT Quick Coupled Transcription/Translation System (Promega, Madison, WI). Approximately 5 μ g of purified GST and its fusion proteins coupled on agarose beads were mixed with 5 μ l of *in vitro* translated probe with gentle rotation at 4 °C overnight in a binding buffer (20 mM HEPES [pH 7.7], 75 mM KCl, 0.1 mM EDTA, 2.5 mM MgCl₂, 0.05% Nonidet P-40, 1 mM dithiothreitol, and 0.1 mM methionine) supplemented with 10 mg/ml bovine serum albumin (BSA) and 1% protease inhibitor cocktail (Roche, Mannheim, Germany). The beads were washed 3 times with fresh binding buffer, collected by centrifugation at 3,000 rpm for 5 minutes, and the bound probes were released by boiling in SDS sample buffer and analyzed by SDS-PAGE and autoradiography. For the effects of rifampicin on SMRT-PXR interaction, HA-PXR was overexpressed in HEK293 cells with or without rifampicin treatment. Total cell extracts were prepared and incubated with GST fusion proteins for 16 hours at 4 °C, and analyzed as described above.

Co-Immunoprecipitation - Co-immunoprecipitation was conducted according to a standard procedure using anti-FLAG (M2) agarose beads (Sigma, St. Louis, MO). Whole cell extracts

were prepared from HEK293 cells transfected with indicated plasmids in a lysis buffer (20 mM HEPES [pH7.9], 1 mM EDTA, 1 mM EGTA, 150 mM NaCl, 1 mM dithiothreitol [DTT], and 0.5% Nonidet P-40). The cell extracts (100 µg each) were pre-absorbed with protein A-agarose beads for 1 hour at room temperature before adding the anti-FLAG agarose (30 µl for each reaction). The binding reactions were incubated at 4 °C overnight. The immunoprecipitates were then collected by centrifugation and washed extensively with phosphate-buffered saline containing 0.1% Nonidet P-40. The final precipitates were dissolved in SDS protein sample buffer and analyzed by SDS-PAGE and Western blot. Western blot was conducted using the ECL reagents according to manufacturer's recommendations (GE Healthcare, Buckinghamshire, UK).

Gel Electrophoresis Mobility Shift Assay - Gel electrophoresis mobility shift (gel shift) assay was conducted as previously described (Blumberg et al., 1998; Chen and Evans, 1995a). Briefly, a double-stranded DNA of the DR4-type element of the following sequence: AGC TTA AGA GGT CAC GAA AGG TCA CTC GCA T (where the underlined sequences are the two NR consensus half sites) was labeled with [³²P]-dCTP by standard Klenow fill-in reaction. The radioactive probe was purified using a spin column (Bio-Rad, Foster City, CA). Approximately 5 x 10⁴ dpm (about 1 ng) of the probe was incubated with 1 µL each of the *in vitro* translated hPXR442 and hRXRα443 in a binding buffer (7.5% glycerol, 20 mM Hepes [pH 7.5], 2 mM DTT, 0.1% Nonidet P-40, 1 µg poly (dI-dC), and 100 mM KCl) for 20 min on ice. Approximately 6 µg of the purified GST or GST fusion proteins were added to the reaction for an additional 1-hour at room temperature. The DNA-protein complexes were then separated on a 5% native polyacrylamide gel and analyzed by autoradiography.

Immunofluorescence Microscopy. COS-7 cells were plated on coverglasses in 24-well plates one day prior to transfection. Twenty-four hours after transfection, cells were fixed in a methanol:acetic acid (1:1, v/v) mixture and processed by indirect immunofluorescence staining as previously described (Li et al., 2000). After extensive washing, FITC-conjugated goat anti-rabbit and rhodamine-conjugated goat anti-mouse antibodies were added. The cells were then stained with DAPI (4', 6-diamidino-2-phenylindole dihydrochloride hydrate, Sigma Chemical Co.) and mounted on slides with ProLong Antifade reagents (Molecular Probes, Eugene, OR). Standard epifluorescence microscopy was performed on a Zeiss inverted microscope Axiovert 200 equipped with a cool charge-coupled device camera (AxioCam). The images were captured and analyzed by the Axiovision software (Zeiss, Thornwood, NY).

Cell Culture and Transient Transfection – COS-7 cells were maintained in phenol red-free Dulbecco's modified Eagle's medium (DMEM) supplemented with 10% fetal bovine serum (FBS) and antibiotic (GibcoBRL, Carlsbad, CA). Transient transfection was performed by standard calcium phosphate precipitation method. Human liver HepG2 cells (5×10^5) were seeded in 6-well plates and transfected with FuGENE-6 (Roche Diagnostic, Indianapolis, IN). After transfection, cells were washed with phosphate-buffered saline and re-fed with fresh medium containing vehicle (DMSO) or vehicle plus 10 μ M of rifampicin (where indicated). Luciferase activity was measured by plate luminometer and normalized with β -galactosidase activity as previously described (Zhang et al., 2004).

Real-time PCR

Paired cDNAs from various human normal and tumor samples were purchased from BioChain Institute (Hayward, CA). Normal mouse and human liver cDNA libraries were purchased from Clontech. Total RNA was also isolated from cell lines COS-7, HeLa, HepG2, A549, HEK293 and CV-1 cells using Trizol reagents (Invitrogen, Rockville, MD). First-strand cDNA was synthesized from 2 μ g of total RNA using poly-T primers (200 ng) and Superscript III reverse transcriptase. Approximately 50-100 ng of cDNA template was mixed with SYBR[®] Green PCR Master Mix (Applied Biosystems, Foster City, CA) and PCR reactions were performed in an ABI PRISM[®] 7900HT Sequence Detection System (Applied Biosystems). The following primers were used to detect SMRT α , SMRT τ and endogenous control β -actin, respectively:

5'-CGG CTC ATG GGT GGC -3' (upstream primer) and 5'-TCC GGC GGT TGC AGT CT -3' (downstream primer), 5'-GCC TGC CCG CTG CTA TG -3' (upstream primer) and 5' -TCC GGC GGT TGC AGT CT -3' (downstream primer), 5'- ACG GCA TCG TCA CCA ACT G -3' (upstream primer) and 5'- GGT TGG CCT TGG GGT TCA -3' (downstream primer).

The amplification program was initiated with a heating step at 95°C for 10 minutes, followed by 40 cycles of 95 °C for 45 seconds, 54 °C for 30 seconds and 72 °C for 1 minute. The program was maintained at 72 °C for another 10 minutes before proceeding to dissociation step, which consisted of 95 °C for 15 seconds, 60 °C for 15 seconds and 95 °C again for 15 seconds. The threshold Ct data was determined with default setting using Applied Biosystems Sequence Detection Software 2.2. Dissociation curve analysis and agarose gel electrophoresis were used to evaluate the specificity of PCR products. Relative quantification of SMRT α versus SMRT τ was normalized to the internal control β -actin and calculated based on the $2^{-\Delta\Delta C_t}$ method. The amplification efficiencies of SMRT α , SMRT τ and the reference β -actin was confirmed to be approximately equal.

RESULTS

PXR Exhibits Preferential Interaction with SMRT α

The two major SMRT isoforms, τ and α , differ only by a 46-aa sequence inserted after the distal ID2 corepressor motif (Fig. 1A). To investigate potential functional differences between them, we constructed corresponding pairs of their C-terminal NR-interacting domains (Fig. 1A), and first compared their interactions with various NRs. In a yeast two-hybrid assay (Fig. 1B), most NRs, including RAR α , CAR, VDR and ROR γ interacted well with both SMRT τ ID1-2 (aa 2107-2379) and SMRT α ID1-2 (aa 2107-2425) with a slight preference toward SMRT τ . Interestingly, PXR displayed a clear preferential interaction with SMRT α ID1-2. Similarly, RXR α also exhibited a SMRT α preference, but its overall bindings to SMRT were much weaker. In addition, PXR displayed no interaction with SMRT ID1 (aa 2107-2187). In contrast, a strong association between RAR α and SMRT ID1 was observed, consistent with our prior finding (Ghosh et al., 2002). These results suggest that different NRs may have different preferences toward these two SMRT isoforms, and that PXR appears to have a unique preference toward SMRT α .

To further investigate the preferential interaction of PXR with SMRT α , we analyzed the relative survivals of transformed Y190 cells on 3AT-containing plates to measure the activation of the second GAL4-dependent HIS3 reporter (Fig. 1C). Cells co-transformed with or without PXR and the indicated SMRT ID1-2 construct were serially diluted and spotted onto -Trp -Leu or -Trp -Leu -His +3AT plates. On the -Trp -Leu plate, all transformed cells survived equally well, indicating comparable transformation efficiencies and growth rates. However, only cells that were co-transformed with PXR and SMRT showed clear survivals on the 3AT-containing plate, with

SMRT α co-transformed cells displaying better survivals than SMRT τ co-transformed cells. These results support the preferential interaction of PXR with SMRT α .

Next, we asked whether the SMRT α preference by PXR could be recapitulated by *in vitro* binding assay. GST pull-down assays were conducted with GST and GST-SMRT ID1, SMRT τ S1/2 (aa 2077-2471), and SMRT α S1/2 (aa 2077-2517) to pull-down [³⁵S]-labeled PXR and other NRs (Fig. 1D). The amounts of intact GST-SMRT τ S1/2 and GST-SMRT α S1/2 fusion proteins were comparable as revealed by Coomassie blue staining (Fig. 1E), while the amount of GST-SMRT ID1 was slightly more. In this assay, we found again that PXR bound better to SMRT α than SMRT τ , while it displayed no interaction with SMRT ID1. Consistently, RAR α interacted equally well with SMRT ID1, SMRT τ S1/2, and SMRT α S1/2. Similar to PXR, RXR443 failed to bind SMRT ID1, but it interacted weakly with the S1/2 constructs with a preference toward SMRT α . In contrast, while CAR, TR β , and FXR failed to interact with SMRT ID1, these receptors interacted about equally with the S1/2 fragments of both SMRT α and SMRT τ . These results indicate that the preferential interaction of PXR with SMRT α also occurs *in vitro*.

PXR needs to form heterodimers with RXR on DNA elements in order to regulate target gene expression. If SMRT α plays a more important role than SMRT τ in regulating PXR activity, we anticipated that SMRT α should also interact with PXR-RXR-DNA complexes better than SMRT τ . This was tested by gel shift assay using *in vitro* translated receptors, [³²P]-labeled DR4 element, and purified GST-SMRT S1/2 fusion proteins (Fig. 1F). Since the receptor's AF2-helix is known to reduce corepressor binding (Liu et al., 2004), AF2-deletion mutants of both PXR (PXR422) and RXR (RXR443) were utilized in these binding reactions. We found that the S1/2 fragments of

both SMRT τ and SMRT α were capable of interacting with the PXR-RXR-DR4 complex in the gel shift assay. Intriguingly, SMRT α again showed a more efficient binding to the PXR-RXR-DNA complex than SMRT τ , suggesting that the SMRT α preference also occurs at the level of receptor-DNA complex.

Finally, we tested whether the SMRT α preference for PXR also occurs in mammalian cells. Co-immunoprecipitation assay was conducted using HEK293 cell extracts transfected with HA-PXR and FLAG-cSMRT τ (aa 2095-2471) or FLAG-cSMRT α (aa 2095-2517) (Fig. 1G). Cell extracts were immunoprecipitated by anti-FLAG agarose beads, followed by Western blot detection of PXR. Both PXR and the two SMRT isoforms were expressed at similar levels as shown in the inputs. Remarkably, we found that PXR was preferentially immunoprecipitated with SMRT α by approximately four-fold higher than with SMRT τ (lower panel), suggesting that PXR preferentially interacts with SMRT α also in mammalian cells. Together, these results strongly suggest that PXR interacts preferentially with SMRT α both *in vitro* and *in vivo*.

SMRT α -PXR Interaction Is Resistant to Ligand-induced Dissociation

We have previously shown that the interaction of PXR with SMRT τ could be disrupted by PXR agonists (Johnson et al., 2006); thus, it is interesting to test whether the interaction of PXR with SMRT α is also sensitive to PXR ligands. A series of corresponding SMRT τ/α constructs were compared for their interactions with PXR and their responses to PXR ligands by yeast two-hybrid assay (Fig. 2A). Under conditions where PXR had little interaction with SMRT ID1, SMRT τ ID2 (aa 2284-2379), or cN-CoR (aa 1929-2440), strong associations of PXR with SMRT α ID2 (aa 2284-2425), SMRT τ ID1-2, and SMRT α ID1-2 were observed in the absence of ligand (Fig. 2A).

This suggests that SMRT α ID2 is the preferred binding site for PXR, consistent with our prior observation (Johnson et al., 2006). Also consistently, the human PXR-specific ligands rifampicin (Rif) and clotrimazole (CTZ) diminished PXR's interaction with SMRT τ ID1-2, whereas the mouse PXR-specific ligand pregnolone-16 α -carbonitrile (PCN) had little or no effect. Remarkably, none of these PXR ligands were capable of diminishing PXR's association with SMRT α ID2 or SMRT α ID1-2. These results suggest that SMRT α also differs from SMRT τ in a way that its interaction with PXR is resistant to ligand-induced dissociation.

To investigate the resistancy of SMRT α -PXR complex to ligand-induced dissociation in greater detail, we compared the effects of rifampicin on PXR's interactions with SMRT τ ID1-2, SMRT α ID1-2, and RAC3 (aa 1-1204) in a ligand concentration-dependent manner (Fig. 2B). Consistent with a prior finding (Johnson et al., 2006), rifampicin disrupted the SMRT τ -PXR interaction, while concomitantly enhanced the RAC3-PXR interaction. In contrast, the SMRT α -PXR interaction remained strong at all concentrations of rifampicin, suggesting that the SMRT α -PXR complex is indeed resistant to rifampicin.

To recapitulate the ligand resistancy of SMRT α -PXR interaction *in vitro*, we conducted GST pull-down assay using HA-PXR expressed in mammalian cells and treated with rifampicin. Purified GST and GST fusions of SMRT ID1, SMRT τ S1/2, and SMRT α S1/2 were mixed with cell extracts containing unliganded or rifampicin-bound HA-PXR, and the bound PXR was detected by Western blot (Fig. 2C). With solvent alone, we found that both SMRT τ S1/2 and SMRT α S1/2 pulled down significant amounts of HA-PXR, while GST and GST-SMRT ID1 could not. Consistently, SMRT α pulled down more PXR than SMRT τ . Intriguingly, rifampicin

disrupted PXR's interaction with SMRT τ , whereas it had only minimal effect on the interaction with SMRT α . These results suggest that, in contrast to SMRT τ , SMRT α is capable of binding with PXR in the presence of rifampicin.

Lastly, we analyzed the effects of rifampicin on colocalization of PXR with SMRT in mammalian cells (Fig. 2D). Full-length SMRT τ is known to accumulate at nuclear foci (Park et al., 1999). EGFP-SMRT τ also formed nuclear foci and displayed colocalization with PXR at those foci, similar to a prior finding (Johnson et al., 2006). Interestingly, rifampicin treatment caused a clear dissociation of PXR from SMRT τ nuclear foci, whereas SMRT foci themselves were not affected. Similarly, EGFP-SMRT α also formed nuclear foci and colocalized efficiently with PXR in the absence of ligand. Surprisingly, rifampicin was unable to release PXR from these SMRT α foci, suggesting that the association of PXR with SMRT α in mammalian cells is also resistant to ligand-induced dissociation. Taken together, these results strongly suggest that the PXR-SMRT α complex is resistant to ligand-induced dissociation both *in vitro* and *in vivo*.

PXR Transcriptional Activity Is Preferentially Inhibited by SMRT α

As SMRT α displays distinct properties from SMRT τ in terms of interacting with PXR and its ligand sensitivity, it was of interests to compare their abilities on suppressing PXR transcriptional activity. To do so, we used a cell-based assay with a CYP3A4 promoter-driven luciferase reporter activated by rifampicin in the presence of PXR. We found that both SMRT τ and SMRT α were capable of suppressing reporter gene activity in a concentration-dependent manner in COS-7 (Fig. 3A) and HepG2 cells (Fig. 3B). Intriguingly, SMRT α exhibited a stronger inhibitory effect on PXR's transcriptional activity than SMRT τ at all concentrations in both cell

types. Furthermore, SMRT α also exhibited a stronger corepressor activity than SMRT τ on a GAL4-dependent luciferase reporter MH100-tk-luc in a GAL4-PXR-dependent manner (Fig. 3C). As a control, we found that SMRT α had little effect on the expression of MH100-tk-luc reporter in the presence of GAL4 DBD alone. Both full-length SMRT α and SMRT τ were expressed at similar levels in the transfected cells as detected by Western blot (Fig. 3D). Together, these results indicate that SMRT α has a stronger inhibitory effect than SMRT τ on PXR-mediated transcriptional activity.

SMRT α and SMRT τ Possess Comparable Intrinsic Repression Activity

The higher corepressor activity of SMRT α over SMRT τ on PXR is consistent with its higher PXR binding affinity and the resistancy to ligand-induced dissociation. However, the corepressor function could also be affected by intrinsic basal transcription repression activity. To address this possibility, we compared the basal transcriptional potentials between SMRT α and SMRT τ using GAL4 DBD fusion proteins on the GAL4-dependent MH100-tk-luc reporter. In this assay, we found that GAL4-SMRT τ (full-length) and GAL4-SMRT α (full-length) exhibited strong repression activity at similar levels (Fig. 4A), suggesting that these SMRT isoforms have similar potentials in repressing basal transcription. Furthermore, SMRT τ is known to accumulate at discrete nuclear foci where it colocalizes with HDACs (Privalsky, 2001; Wu et al., 2001). Immunostaining of co-expressed EGFP-SMRT α (full-length) and FLAG-SMRT τ shows that these two proteins colocalized at discrete nuclear foci (Fig. 4B), suggesting that SMRT α has similar distribution as SMRT τ . In addition, we found that EGFP-SMRT α also efficiently recruited HDAC4 to these nuclear foci, suggesting that SMRT α also interact with HDACs. These results suggest that SMRT α and SMRT τ have comparable intrinsic repression activities; therefore, the

differences in their abilities to inhibit PXR cannot be attributed to differences in their repression potentials.

Determinants of SMRT α Preferential Binding by PXR

We have previously shown that SMRT τ interacts with PXR through its ID2 domain (Johnson et al., 2006; Wang et al., 2006). Similarly, SMRT α seems to utilize the ID2 domain for PXR interaction as well, because the ID1 domain alone does not interact with PXR while the ID1-2 fragment of SMRT α does (Fig. 1 and 2). The only difference between SMRT α and SMRT τ is the α -specific 46-aa insert after residue G2352, immediately downstream from the ID2's "LEAIIRKAL" core motif (Fig. 5A). Therefore, this 46-aa sequence must be involved in the enhanced binding of SMRT α by PXR. To investigate how this 46-aa sequence enhances interaction with PXR, we first hypothesized that this 46-aa insert might enable the ID1 domain to interact with PXR, thus creating two binding sites. This was tested by measuring PXR's interactions with a series of point mutations on GST-SMRT α S1/2 by GST pull-down assay (Fig. 5B). The wild type GST-SMRT α S1/2 and its mutants were expressed, purified, and confirmed by Coomassie blue staining (Fig. 5B, right). Intriguingly, we found that only the ID2 mutation (mID2, or I2345A/I2346A), but not the ID1 mutation (mID1, or V2142A/I2143A) or the two non-ID mutations (m3 and m4), disrupted SMRT α 's interaction with PXR. The ID1 and ID2 double mutation (mID1-2) also disrupted PXR binding. In contrast, mID1, but not mID2 mutation diminished SMRT α 's interaction with RAR α . These results suggest that PXR still interacts with SMRT α through its ID2 domain, thus the 46-aa insert does not enable ID1 to interact with PXR. Therefore, the enhanced interaction of SMRT α is likely mediated directly through the ID2 motif and the 46-aa sequence.

In the SMRT τ sequence, a methionine and four consecutive glycine residues follow the ID2 core motif immediately. Glycine has no side chain and therefore can adopt different conformations. It frequently occurs in turns of proteins and is sometimes known as “helix breaker”. Therefore, we replaced the first three glycines in the SMRT τ sequence with alanines, to extend, theoretically, the length of the ID2 corepressor helix (Fig. 5C, SMRT τ 3G/A mutant). However, this mutation was ineffective in enhancing PXR’s interaction with SMRT τ ID1-2 (Fig. 5D), suggesting that a mere extension of the ID2 helix is not sufficient to enhance PXR interaction. Hence, we hypothesized that the 46-aa sequence might participate directly in stabilizing the ID2-PXR interaction, or by providing an additional binding surface for PXR. The potential contribution of these 46 amino acids to PXR’s interaction was analyzed first by deletion analysis. First, we confirmed that deletion of the entire 46-aa insert from SMRT α (Δ 46 mutant) converted its PXR binding efficiency to the level of SMRT τ (Fig. 5D, left panel). Surprisingly, deletion of the first 5 (Δ 5) or 10 (Δ 10) amino acids of the 46-aa insert was each sufficient to reduce SMRT α ’s interaction to the level of SMRT τ . Conversely, deletion of the C-terminal 36 (Δ 36c) or 41 amino acids (Δ 41c) had little effect on SMRT α ’s interaction with PXR. These results clearly suggest that the first five amino acids (KYDQW) of the 46-aa insert are necessary and sufficient for the preferential interaction of SMRT α with PXR.

To further pinpoint the exact residues that are responsible for the enhanced SMRT α interaction with PXR, we conducted site-directed mutagenesis on the above five amino acids. Interestingly, we found that replacement of the first three residues from KYD to AAA was sufficient to reduce the SMRT α -PXR interaction to the level of SMRT τ (Fig. 5D, right panel). Additional mutational

analysis showed that the K2353 to alanine mutation (K2353A) had no effect, while the Y2354 to alanine mutation (Y2354A) completely abolished the enhanced interaction. In contrast, mutation of D2355 to alanine (D2355A) caused a partial decline in the SMRT α -PXR interaction. These results indicate that amino acids Y2354 and D2355 are both involved and critical for the preferential association of SMRT α by PXR.

Expression of SMRT Isoforms in Human Tissues and Cancer Cells

To shed light into potential physiological relevance of the SMRT isoforms, we decided to compare the relative expression levels of SMRT α versus SMRT τ in various human tissues and cancer cell lines. Paired normal versus tumor cDNAs from various human tissues, and cDNAs generated from established cell lines, were amplified by real-time PCR using a set of primers that specifically amplify either SMRT α or SMRT τ . Dissociation curve analysis showed a specific peak at the predicted melting temperature of each amplified PCR product. Electrophoresis on a 1.8% agarose gel confirmed the specificity of the same PCR product with one single band at the expected size. In this experiment, we found that SMRT α is the predominant form expressed in both normal and tumor tissues of the breast, kidney and prostate (Fig. 6A, B). In particular, the normal prostate appears to express the highest level of SMRT α (Fig. 6B). Interestingly, while SMRT α remained as the dominant form in the tumor samples of liver, SMRT τ was more abundant in normal liver tissue (Fig. 6B). Additionally, SMRT α is also the major form expressed in several established cell lines (Fig. 6C).

DISCUSSION

The xenobiotic receptor PXR plays an important role in the metabolism of many prescribed drugs by controlling expression of many drug-metabolizing enzymes in liver. In this study, we have compared the roles of two different SMRT isoforms, α and τ , in regulating PXR activity. We found that PXR preferentially interacts with the α isoform in a ligand-resistant manner, and that SMRT α represses PXR activity more efficiently in comparison to SMRT τ . We further uncovered the amino acid residues that are responsible for PXR preferential binding to SMRT α . In addition, we found that SMRT α is the dominant isoform expressed in several human tissues and cancer cell lines, suggesting an important role for SMRT α in regulating PXR activation.

There are two distinct corepressor motifs in the SMRT sequence that exhibit different binding affinities toward different NRs. For instance, TR interacts with both the upstream ID1 motif and the downstream ID2, while RAR interacts primarily with ID1, although PXR and RXR apparently prefer the ID2 (Ghosh et al., 2002; Johnson et al., 2006). Since the SMRT α -specific 46-aa sequence is located immediately after the ID2 LxxIIxxxL core motif, it is reasonable to speculate that this 46-aa sequence might affect the binding of ID2 to other proteins. Our data suggest that the 46-aa sequence does not contain additional interacting surface for PXR, nor does it enable PXR-ID1 interaction (Fig. 5). Interestingly, SMRT α reportedly interacted better with TRs on DNA *in vitro* (Goodson et al., 2005). Although this difference was not seen in our assay (Fig. 1), it remains possible that the presence of DNA might influence SMRT isoform preference. However, if TR does possess differential affinity toward SMRT isoforms, the difference may not be as profound as for PXR. Our previous structural modeling of the PXR LBD-SMRT ID2 complex (Wang et al., 2006) was unable to address the involvement of the 46-aa insert, because of its length

and distance from the ID2 core motif. Future improvement in our modeling system will be informative to predict any molecular interaction with PXR involving the 46-aa sequence.

In contrast to ligand-reversible association of SMRT τ with PXR, SMRT α retains a strong interaction with PXR in the presence of PXR ligands (Fig. 2). It is known that certain NR variants possess ligand-irreversible association with SMRT (Tagami et al., 1998). Our current data further suggest that different SMRT isoforms may have different affinity toward the same receptor. In addition to the ligand-irreversible effect, several other possibilities may also explain the preferential inhibition of PXR by SMRT α . For example, in the presence of SMRT α , rifampicin might be unable to produce a conformational change in PXR that is required to release the corepressor. Alternatively, SMRT α might prevent rifampicin from binding to PXR. Equally possible, the presence of SMRT α might interfere with the ability of PXR to recruit coactivators.

To shed light into the relative importance of SMRT isoforms on regulating PXR activity, we compared the expression of SMRT α vs. SMRT τ in various human tissues and cancer cell lines (Fig. 6). Surprisingly, SMRT α was found at higher levels than SMRT τ in most tissues and cell lines, especially in the normal prostate. Exceptionally, SMRT τ was found higher in normal liver sample (Fig. 6A, B). While both SMRT α and SMRT τ are ubiquitously expressed and the amount of SMRT α in normal liver tissue is slightly lower than in other tested tissues, but the amount of SMRT τ in normal liver is much higher comparing to other tissues. It is important to note that human PXR is most abundantly expressed in liver and intestine (Blumberg et al., 1998; Lehmann et al., 1998). Since the interaction between PXR and SMRT τ is sensitive to PXR ligand-induced dissociation, and SMRT τ is more abundant than SMRT α in normal liver tissue, it is possible that

the PXR-SMRT τ interaction may be more relevant for the inductive response of PXR activation by ligands in the liver. Furthermore, we speculate that the relatively more abundant SMRT α in other tissues and cancerous samples and cell lines might play a role in limiting PXR activation in these other tissues, because the PXR-SMRT α interaction is stronger and more resistant to ligand-induced dissociation.

PXR coordinately regulates drug clearance in response to a wide variety of xenobiotic compounds; thus, reducing PXR activity may diminish drug clearance and increase the potency of therapeutic drugs, causing dangerous drug-drug interaction. There has been a great amount of interests on drug discovery with emphasis on understanding structure-function relationship for attenuating drug-mediated PXR activation (Gao et al., 2007; Ung et al., 2007). The fact that the key amino acids of the SMRT α -specific 46-aa insert is located within the first five amino acids, which is only two residues away from the ID2 core sequence, may provide a novel therapeutic target utilizing an extended ID2 motif via a peptide interference mechanism. Indeed, the SMRT corepressor motif has been designed as a peptide to occupy the lateral groove of BCL6 and compete with corepressor binding (Polo et al., 2004). These peptides not only attenuate BCL6-mediated transcriptional repression, but also reactivate expression of BCL6 target genes, resulting in disruption of endogenous BCL6 repression complexes. Thus, this current study may provide a molecular basis for rational drug designs aimed at enhancing the efficacy of therapeutic drugs by inhibiting PXR-mediated drug metabolism.

ACKNOWLEDGMENTS

We thank Martin L. Privalsky at U.C. Davis, California for providing the pGEX-SMRT τ S1/2 (aa 2077-2471) and pGEX-SMRT α S1/2 (aa 2077-2517) plasmid vectors.

REFERENCES

- Blumberg B, Sabbagh W, Jr., Juguilon H, Bolado J, Jr., van Meter CM, Ong ES and Evans RM (1998) SXR, a novel steroid and xenobiotic-sensing nuclear receptor. *Genes & development* **12**(20):3195-3205.
- Chen JD and Evans RM (1995a) A transcriptional co-repressor that interacts with nuclear hormone receptors. *Nature* **377**(6548):454-457.
- Chen JD and Evans RM (1995b) A transcriptional co-repressor that interacts with nuclear hormone receptors [see comments]. *Nature* **377**(6548):454-457.
- Falkner KC, Pinaire JA, Xiao GH, Geoghegan TE and Prough RA (2001) Regulation of the rat glutathione S-transferase A2 gene by glucocorticoids: involvement of both the glucocorticoid and pregnane X receptors. *Molecular pharmacology* **60**(3):611-619.
- Gao YD, Olson SH, Balkovec JM, Zhu Y, Royo I, Yabut J, Evers R, Tan EY, Tang W, Hartley DP and Mosley RT (2007) Attenuating pregnane X receptor (PXR) activation: a molecular modelling approach. *Xenobiotica* **37**(2):124-138.
- Geick A, Eichelbaum M and Burk O (2001) Nuclear receptor response elements mediate induction of intestinal MDR1 by rifampin. *J Biol Chem* **276**(18):14581-14587.
- Ghosh JC, Yang X, Zhang A, Lambert MH, Li H, Xu HE and Chen JD (2002) Interactions that determine the assembly of a retinoid X receptor/corepressor complex. *Proc Natl Acad Sci U S A* **99**(9):5842-5847.
- Goodson ML, Jonas BA and Privalsky ML (2005) Alternative mRNA Splicing of SMRT Creates Functional Diversity by Generating Corepressor Isoforms with Different Affinities for Different Nuclear Receptors. *J Biol Chem* **280**(9):7493-7503.

- Guenther MG, Lane WS, Fischle W, Verdin E, Lazar MA and Shiekhattar R (2000) A core SMRT corepressor complex containing HDAC3 and TBL1, a WD40- repeat protein linked to deafness. *Genes & development* **14**(9):1048-1057.
- Harmsen S, Meijerman I, Beijnen JH and Schellens JH (2007) The role of nuclear receptors in pharmacokinetic drug-drug interactions in oncology. *Cancer Treat Rev* **33**(4):369-380.
- Horlein AJ, Naar AM, Heinzl T, Torchia J, Gloss B, Kurokawa R, Ryan A, Kamei Y, Soderstrom M, Glass CK and et al. (1995) Ligand-independent repression by the thyroid hormone receptor mediated by a nuclear receptor co-repressor. *Nature* **377**(6548):397-404.
- Hu X and Lazar MA (1999) The CoRNR motif controls the recruitment of corepressors by nuclear hormone receptors. *Nature* **402**(6757):93-96.
- Johnson DR, Li CW, Chen LY, Ghosh JC and Chen JD (2006) Regulation and binding of pregnane X receptor by nuclear receptor corepressor silencing mediator of retinoid and thyroid hormone receptors (SMRT). *Mol Pharmacol* **69**(1):99-108.
- Kast HR, Goodwin B, Tarr PT, Jones SA, Anisfeld AM, Stoltz CM, Tontonoz P, Kliewer S, Willson TM and Edwards PA (2002) Regulation of multidrug resistance-associated protein 2 (ABCC2) by the nuclear receptors pregnane X receptor, farnesoid X-activated receptor, and constitutive androstane receptor. *J Biol Chem* **277**(4):2908-2915.
- Kliewer SA, Moore JT, Wade L, Staudinger JL, Watson MA, Jones SA, McKee DD, Oliver BB, Willson TM, Zetterstrom RH, Perlmann T and Lehmann JM (1998) An orphan nuclear receptor activated by pregnanes defines a novel steroid signaling pathway. *Cell* **92**(1):73-82.
- Kodama S, Koike C, Negishi M and Yamamoto Y (2004) Nuclear receptors CAR and PXR cross talk with FOXO1 to regulate genes that encode drug-metabolizing and gluconeogenic enzymes. *Molecular and cellular biology* **24**(18):7931-7940.

- Lehmann JM, McKee DD, Watson MA, Willson TM, Moore JT and Kliewer SA (1998) The human orphan nuclear receptor PXR is activated by compounds that regulate CYP3A4 gene expression and cause drug interactions. *J Clin Invest* **102**(5):1016-1023.
- Leo C and Chen JD (2000) The SRC family of nuclear receptor coactivators. *Gene* **245**(1):1-11.
- Li H, Leo C, Zhu J, Wu X, O'Neil J, Park EJ and Chen JD (2000) Sequestration and inhibition of Daxx-mediated transcriptional repression by PML. *Molecular and cellular biology* **20**(5):1784-1796.
- Liu H, Shaw CK, Reineke EL, Liu Y and Kao HY (2004) Retinoid X receptor alpha (RXRalpha) helix 12 plays an inhibitory role in the recruitment of the p160 co-activators by unliganded RXRalpha/retinoic acid receptor alpha heterodimers. *J Biol Chem* **279**(43):45208-45218.
- Moore JT, Moore LB, Maglich JM and Kliewer SA (2003) Functional and structural comparison of PXR and CAR. *Biochim Biophys Acta* **1619**(3):235-238.
- Muangmoonchai R, Smirlis D, Wong SC, Edwards M, Phillips IR and Shephard EA (2001) Xenobiotic induction of cytochrome P450 2B1 (CYP2B1) is mediated by the orphan nuclear receptor constitutive androstane receptor (CAR) and requires steroid co-activator 1 (SRC-1) and the transcription factor Sp1. *Biochem J* **355**(Pt 1):71-78.
- Nagy L, Kao HY, Chakravarti D, Lin RJ, Hassig CA, Ayer DE, Schreiber SL and Evans RM (1997) Nuclear receptor repression mediated by a complex containing SMRT, mSin3A, and histone deacetylase. *Cell* **89**(3):373-380.
- Ordentlich P, Downes M, Xie W, Genin A, Spinner NB and Evans RM (1999) Unique forms of human and mouse nuclear receptor corepressor SMRT. *Proc Natl Acad Sci U S A* **96**(6):2639-2644.

- Park EJ, Schroen DJ, Yang M, Li H, Li L and Chen JD (1999) SMRTE, a silencing mediator for retinoid and thyroid hormone receptors- extended isoform that is more related to the nuclear receptor corepressor. *Proc Natl Acad Sci U S A* **96**(7):3519-3524.
- Polo JM, Dell'Oso T, Ranuncolo SM, Cerchietti L, Beck D, Da Silva GF, Prive GG, Licht JD and Melnick A (2004) Specific peptide interference reveals BCL6 transcriptional and oncogenic mechanisms in B-cell lymphoma cells. *Nat Med* **10**(12):1329-1335.
- Privalsky ML (2004) The role of corepressors in transcriptional regulation by nuclear hormone receptors. *Annual review of physiology* **66**:315-360.
- Privalsky MLRN (2001) Regulation of SMRT and N-CoR corepressor function. *Curr Top Microbiol Immunol* **254**:117-136.
- Synold TW, Dussault I and Forman BM (2001) The orphan nuclear receptor SXR coordinately regulates drug metabolism and efflux. *Nat Med* **7**(5):584-590.
- Tagami T, Kopp P, Johnson W, Arseven OK and Jameson JL (1998) The thyroid hormone receptor variant alpha2 is a weak antagonist because it is deficient in interactions with nuclear receptor corepressors. *Endocrinology* **139**(5):2535-2544.
- Toell A, Kroncke KD, Kleinert H and Carlberg C (2002) Orphan nuclear receptor binding site in the human inducible nitric oxide synthase promoter mediates responsiveness to steroid and xenobiotic ligands. *J Cell Biochem* **85**(1):72-82.
- Ung CY, Li H, Yap CW and Chen YZ (2007) In silico prediction of pregnane X receptor activators by machine learning approaches. *Mol Pharmacol* **71**(1):158-168.
- Urquhart BL, Tirona RG and Kim RB (2007) Nuclear receptors and the regulation of drug-metabolizing enzymes and drug transporters: implications for interindividual variability in response to drugs. *J Clin Pharmacol* **47**(5):566-578.

- Wang CY, Li CW, Chen JD and Welsh WJ (2006) Structural Model Reveals Key Interactions in the Assembly of the Pregnane X Receptor/Corepressor Complex. *Mol Pharmacol*.
- Watkins RE, Wisely GB, Moore LB, Collins JL, Lambert MH, Williams SP, Willson TM, Kliewer SA and Redinbo MR (2001) The human nuclear xenobiotic receptor PXR: structural determinants of directed promiscuity. *Science (New York, NY)* **292**(5525):2329-2333.
- Westin S, Rosenfeld MG and Glass CK (2000) Nuclear receptor coactivators. *Adv Pharmacol* **47**:89-112.
- Wipf P, Gong H, Janjic JM, Li S, Day BW and Xie W (2007) New opportunities for pregnane X receptor (PXR) targeting in drug development. lessons from Enantio- and species-specific PXR ligands identified from a discovery library of amino acid analogues. *Mini Rev Med Chem* **7**(6):617-625.
- Wu X, Li H and Chen JD (2001) The human homologue of the yeast DNA repair and TFIID regulator MMS19 is an AF-1-specific coactivator of estrogen receptor. *J Biol Chem* **276**(26):23962-23968.
- Xu HE, Stanley TB, Montana VG, Lambert MH, Shearer BG, Cobb JE, McKee DD, Galardi CM, Plunket KD, Nolte RT, Parks DJ, Moore JT, Kliewer SA, Willson TM and Stimmel JB (2002) Structural basis for antagonist-mediated recruitment of nuclear co-repressors by PPARalpha. *Nature* **415**(6873):813-817.
- Zhang A, Yeung PL, Li CW, Tsai SC, Dinh GK, Wu X, Li H and Chen JD (2004) Identification of a novel family of ankyrin repeats containing cofactors for p160 nuclear receptor coactivators. *J Biol Chem* **279**(32):33799-33805.

FOOTNOTE

This work was made possible by grant award DK52542 from the National Institutes of Health. Its contents are solely the responsibility of the authors and do not necessarily represent the official views of the funding agency. Current address: The University of Texas, MD Anderson Cancer Center, Houston, Texas (C.-W.L.).

FIGURE LEGENDS

Fig. 1. PXR Interacts Preferentially with SMRT α . (A) Schematic diagrams of various SMRT τ and SMRT α constructs used in this study. The proximal ID1 and distal ID2 corepressor motifs are indicated by black bars, with motif core sequences shown on top. The SMRT α -specific 46-aa insert is shown in grey. The amino acid positions of individual fragments are labeled numerically. (B) PXR interacts preferentially with SMRT α in a yeast two-hybrid assay. The pGBT-hPXR, pAS-hRAR α , pGBT-hRXR α , pGBT-hCAR, pGBT-hVDR, and pGBT-mROR γ were individually transformed into Y190 cells in combination with pACT-SMRT ID1 (aa 2107-2187), pACT-SMRT τ ID1-2 (aa 2107-2379), or pACT-SMRT α ID1-2 (aa 2107-2425). Three colonies from each plate were picked and grown in -Trp -Leu liquid media for 24 hours. The expression of β -galactosidase was measured by liquid ONPG assay after normalization with cell numbers, and average β -galactosidase units were calculated and plotted. (C) Survival assay of yeast cells co-transformed with pGBT-hPXR and pACT-SMRT τ ID1-2 or SMRT α ID1-2 constructs. Indicated numbers of transformed cells were spotted onto -Trp -Leu or -Trp -Leu -His +3AT (50 mM) selection plates and incubated at 30 °C for 2 days. The pGBT9 and pACT2 vectors were used as controls where indicated (-). (D) Interactions of SMRT isoforms with various NRs in GST pull-down assays. *In vitro* translated [³⁵S]-labeled hPXR, hRAR α , hRXR α 443, hCAR, hTR β , and hFXR were incubated with GST, GST-SMRT ID1, GST-SMRT τ S1/2 (aa 2077-2471), or GST-SMRT α S1/2 (aa 2077-2517) at 4 °C overnight. After extensive washing with binding buffer, the bound proteins were collected by centrifugation and analyzed by SDS-polyacrylamide gel electrophoresis and autoradiography. (E) Coomassie blue staining of GST and GST-SMRT fusion proteins used in this study. The GST proteins were purified from

bacteria BL21 cells and analyzed by SDS-PAGE and Coomassie staining. Notable size difference of the intact GST-SMRT ID1, GST-SMRT τ S1/2, and GST-SMRT α S1/2 are marked by asterisks (*). **(F)** Preferential interaction of PXR-RXR heterodimers with SMRT α on a DR4 PXR response element. Gel shift assay was conducted with *in vitro* translated hPXR422, hRXR α 443 and a [³²P]-labeled DR4 element. Equal amount (6 μ g) of purified GST, GST-SMRT τ S1/2, or GST-SMRT α S1/2 were added to individual reaction. The DNA-protein complexes were separated on a native polyacrylamide gel and detected by autoradiography. **(G)** Co-immunoprecipitation of PXR with cSMRT τ/α from mammalian cell extracts. Approximately 1 mg of protein extracts obtained from HEK293 cells co-expressing HA-PXR and FLAG-cSMRT τ (aa 2095-2471) or FLAG-cSMRT α (aa 2095-2517) were immunoprecipitated with monoclonal anti-FLAG antibody-conjugated agarose beads. Approximately 5% of the extract used in each immunoprecipitation reaction (input) was analyzed by Western blot to show the relative amount of HA-PXR and cSMRT τ/α in the cell extracts. The total amount of immunoprecipitates (IP) were analyzed by Western blot with rabbit anti-HA antibody to detect the co-immunoprecipitated HA-PXR. The precipitated HA-PXR in each reaction was quantitated by densitometry and results plotted and shown in the lower panel.

Fig. 2. SMRT α -PXR Interaction Is Resistant to Ligand-Induced Dissociation. **(A)** Effects of PXR ligands on SMRT-PXR interactions in a yeast two-hybrid assay. Yeast colonies co-transformed with pGBT-hPXR and the indicated pACT-SMRT constructs or pACT-cN-CoR were treated with the hPXR-specific ligands rifampicin (Rif, 10 μ M) and clotrimazole (CTZ, 10 μ M), or with the mPXR-specific ligand pregnenolone-16 α -carbonitrile (PCN, 10 μ M) for 48 hours. The empty pACT2 vector was used as a control where indicated (-). The SMRT α ID2 and

SMRT α ID1-2 show stronger, ligand-resistant interactions with PXR in comparison to SMRT τ . **(B)** Rifampicin concentration-dependent dissociation of SMRT τ/α -PXR interaction in a yeast two-hybrid assay. Yeast transformants containing pGBT-hPXR and pACT-SMRT τ ID1-2, pACT-SMRT α ID1-2, or pGAD-RAC3 (1-1204) were grown in -Trp -Leu media for 24 hours. Aliquots of each sample were treated with increasing concentrations of rifampicin (Rif, 10, 25, 50 μ M) and incubated for another 36 hours. Rifampicin had little effect on the interaction of PXR with SMRT α ID1-2, whereas it reduced its interaction with SMRT τ ID1-2 and enhanced interaction with the coactivator RAC3. **(C)** Rifampicin had little effect on the formation of SMRT α -PXR complex. HA-PXR was overexpressed in HEK293 cells in the absence (Sol) or presence of rifampicin (Rif, 10 μ M). Approximately 50 μ g of cell extracts were incubated with 5 μ g of purified GST, GST-SMRT ID1, GST-SMRT τ S1/2 or GST-SMRT α S1/2 for 16 hours at 4 $^{\circ}$ C. The bound HA-PXR proteins were collected by centrifugation and analyzed by SDS-PAGE and Western blot using anti-HA antibody. **(D)** SMRT α colocalizes with PXR in mammalian cells in the presence of rifampicin. COS-7 cells were transfected with pEGFP-hSMRT τ (full-length) or pEGFP-hSMRT α (full-length) together with FLAG-hPXR. Cells were recovered in DMEM media containing 10 μ M of rifampicin or DMSO for 12 hours. Cells were fixed and colocalization between SMRT and PXR were detected by immunostaining with anti-FLAG antibody and the EGFP signals. Rifampicin causes clear dissociation of PXR from SMRT τ nuclear foci, whereas it has little effect or no impact on the SMRT α -PXR colocalization.

Fig. 3. Transcriptional Activity of PXR is Preferentially Suppressed by SMRT α . COS-7 **(A)** and human liver HepG2 **(B)** cells were transiently transfected with pCMXHA-hPXR and

pCYP3A4-tk-luc reporter, together with a β -galactosidase expression vector as an internal control. Increasing amounts of pCMX-FLAG-SMRT α (full-length) or pCMX-FLAG-SMRT τ (full-length) were cotransfected as indicated (in μ g). After transfection, cells were refed with fresh media containing 10 μ M of rifampicin (Rif) where indicated (+) and recovered for 16 hours. Relative fold activations of the reporter in comparison to the control sample without treatment or SMRT co-transfection were determined from three independent experiments. SMRT α inhibits PXR transactivation stronger than SMRT τ in both cell types in a dose-dependent manner. (C) Transcriptional repression by GAL4-PXR is preferentially enhanced by SMRT α . COS-7 cells were transfected with GAL4-hPXR with increasing amounts (in μ g) of pCMX-FLAG-SMRT τ/α (full-length) construct along with the GAL4-dependent MH100-tk-luc reporter and a β -galactosidase control vector. SMRT α did not affect GAL4 activity, while it preferentially enhanced the transcriptional repression activity of GAL-PXR. (D) Western blot analysis showing comparable expression levels of FLAG-SMRT τ/α full-length proteins in the transfected cells.

Fig. 4. SMRT α and SMRT τ Possess Comparable Intrinsic Repression Activities. (A) Transcriptional repressions by GAL4-SMRT α (full-length) and GAL4-SMRT τ (full-length) are comparable. HEK293 cells were transfected with increasing amounts of GAL4 DBD or GAL4 DBD fusions of either full-length SMRT α (GAL4-SMRT α) or full-length SMRT τ (GAL4-SMRT τ), together with a GAL4-dependent MH100-tk-luc reporter. The relative percentages of luciferase activity in comparison to GAL4 DBD alone (set as 100%) were determined from three independent experiments. (B) SMRT α colocalizes with SMRT τ and HDAC4. COS-7 cells were transiently transfected with EGFP-SMRT α (full-length) in

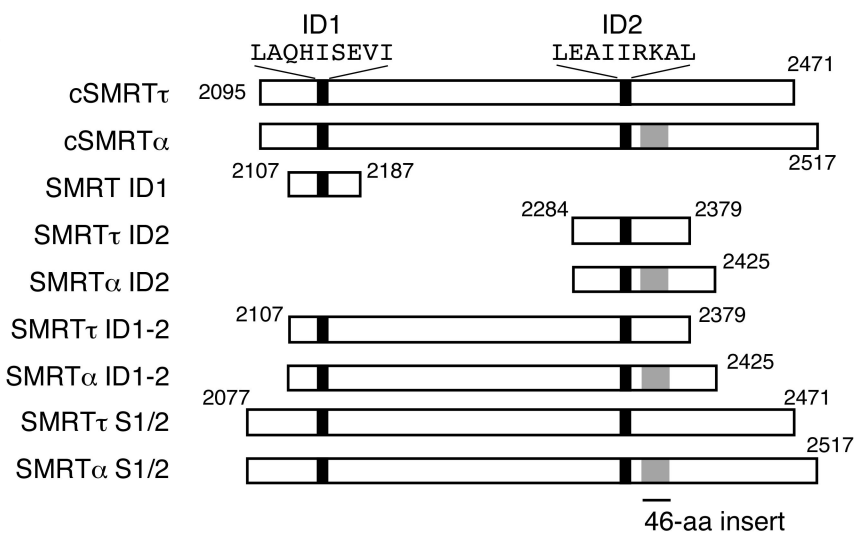
combination with FLAG-SMRT τ (full-length) or FLAG-HDAC4. Transfected cells were fixed and immunostained with anti-FLAG monoclonal antibody and rhodamine-conjugated secondary antibody (red), and visualized in comparison with the EGFP-SMRT α signals. Cell nuclei were stained by DAPI.

Fig. 5. Molecular Determinants of SMRT α Preference for PXR Binding. (A) Sequence of the SMRT α -specific 46 amino acids is shown at the top with the flanking SMRT τ sequences shown at the bottom. This SMRT α -specific sequence is inserted after glycine at position 2352 following the distal ID2 corepressor motif (underlined). The numbers indicate amino acid positions. (B) The ID2 motif mutation in SMRT α disrupts PXR interaction. The wild type (WT) GST-SMRT α S1/2 and its site-directed mutants, mID1 (V2142A/I2143A), mID2 (I2345A/I2346A), mID1-2 (V2142A/I2143A, I2345A/I2346A), m3 (S2285E/K2286E/K2287E), and m4 (L2467A/I2468A), were tested for binding with [³⁵S]-labeled hPXR and hRAR α in a GST pull-down assay. The right panel shows Coomassie blue-stained GST proteins. The mID2-containing mutants (mID2 and mID1-2) show decreased binding to PXR, whereas only mID1-containing mutations (mID1 and mID1-2) affect their interactions with RAR α . (C) Sequence comparison of the SMRT α -specific 46-aa insert and its mutants. The solid line on top marks the 46-aa sequence. Dashed lines represent deletions. The alanine substitutions in the SMRT τ 3G/A and the KYD, K2353A, Y2354A, and D2355A mutants of SMRT α are italicized. The plasmid, pACT-SMRT α ID1-2, was used as a template to construct these mutants used in the following assays. (D) Yeast two-hybrid assays showing interactions of PXR with SMRT α -specific 46-aa-related mutants. Yeast Y190 cells were co-transformed individually with pGBT-hPXR and indicated pACT-SMRT τ/α ID1-2 wild type and indicated mutant constructs.

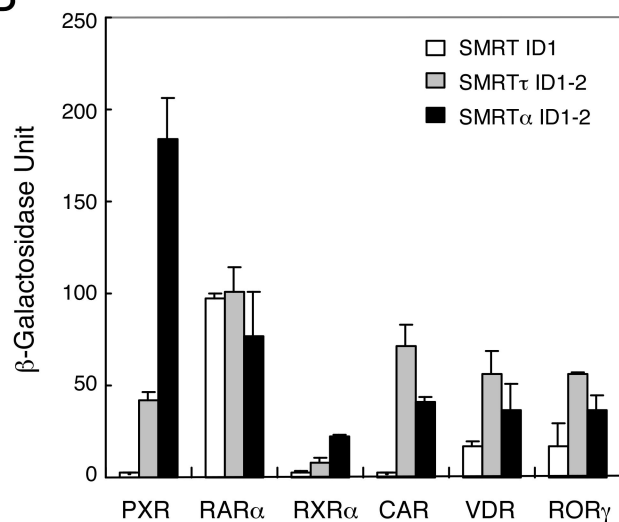
Fig. 6. Expression of SMRT Isoforms in Human Tissues and Cancer Cells. cDNAs from normal (N) and tumor (T) tissues of the breast, kidney, liver and prostate as well as from various established cell lines were amplified using primer sets specific for SMRT α or SMRT τ as described in Materials and Methods. Real time PCR reactions were performed in an ABI PRISM[®] 7900HT Sequence Detection System. Relative quantification of SMRT α versus SMRT τ was normalized to the internal control β -actin and calculated according to the $2^{-\Delta\Delta C_t}$ method. **(A)** SMRT α / τ expression ratios in human normal and tumor tissues. **(B)** Relative abundance of SMRT α and SMRT τ among tested human normal and tumor tissues. **(C)** SMRT α / τ expression ratios in established cell lines.

Figure 1

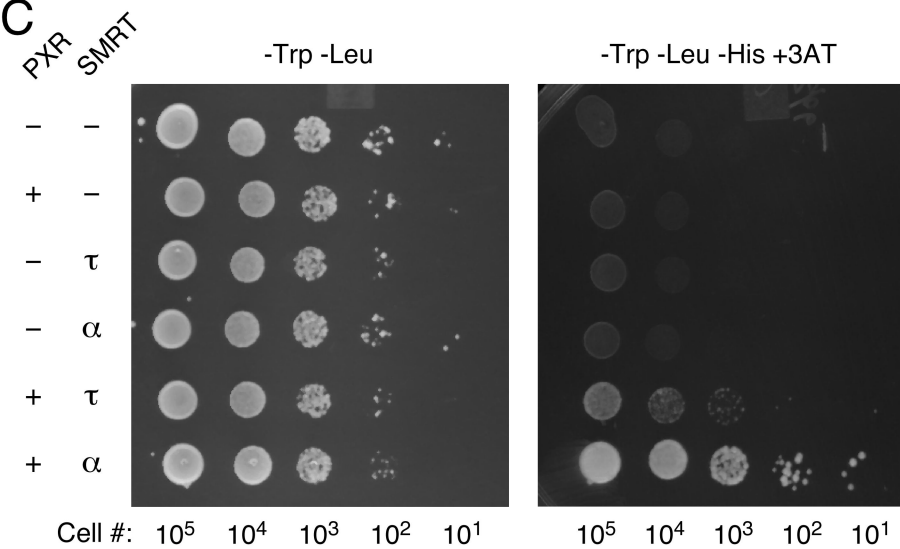
A



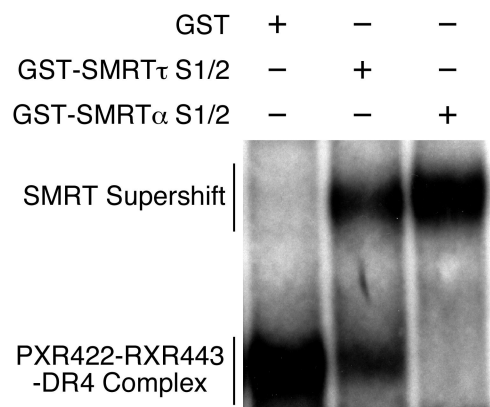
B



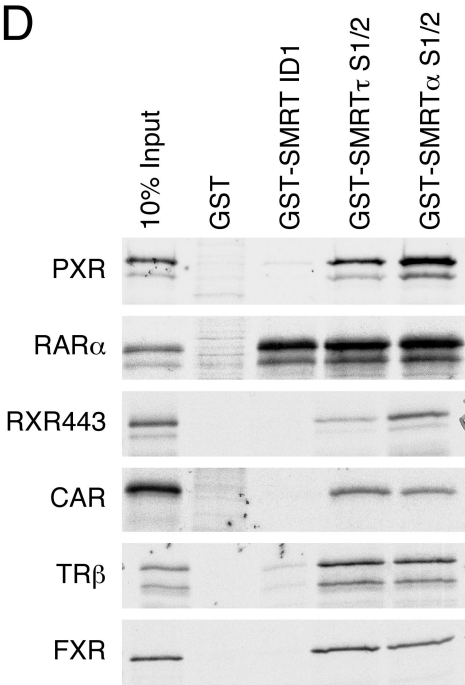
C



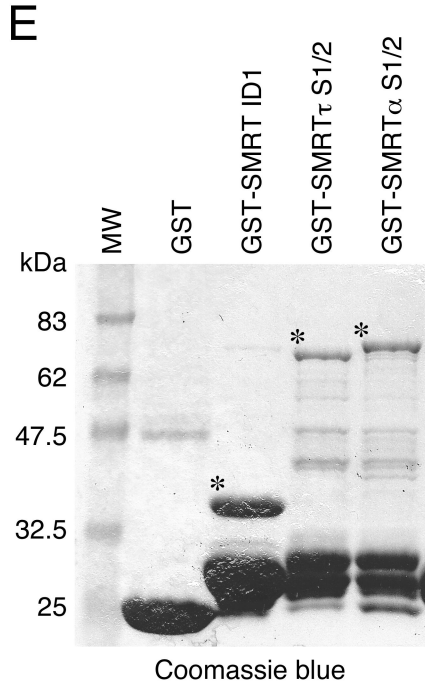
F



D



E



G

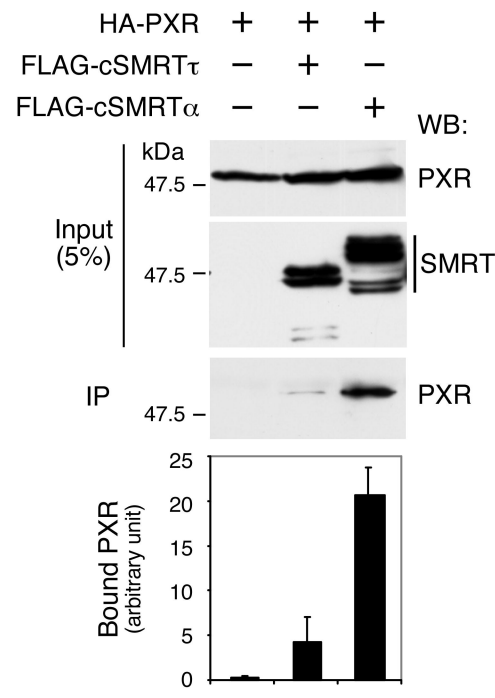
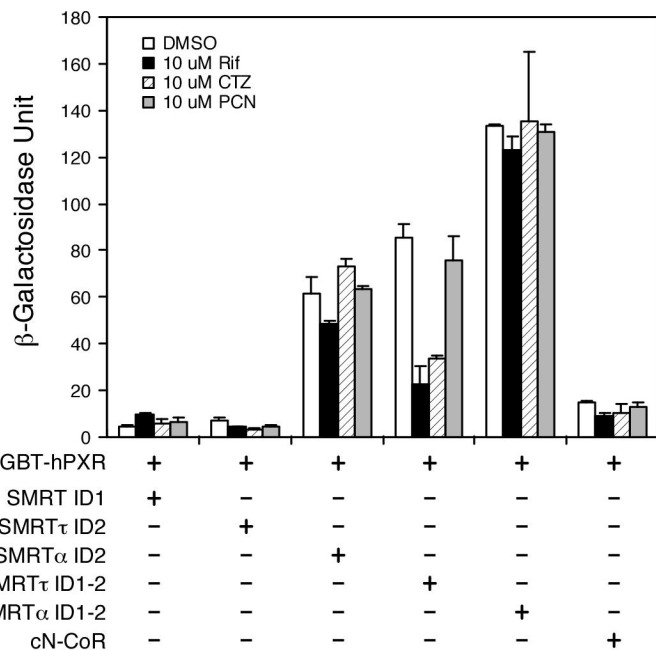
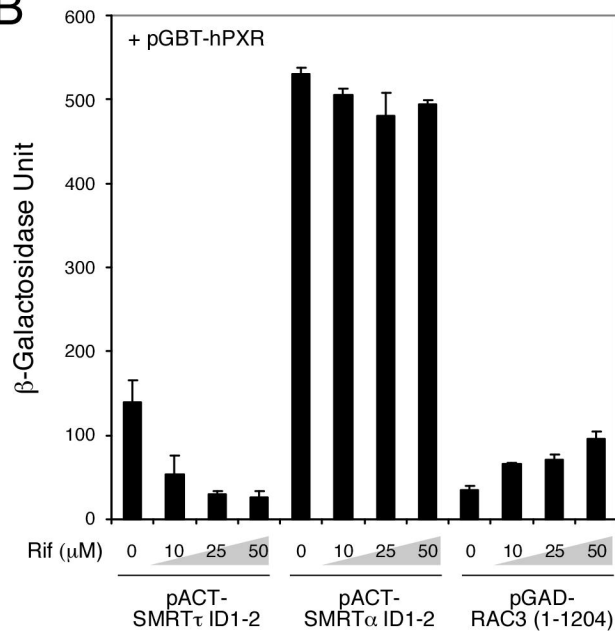


Figure 2

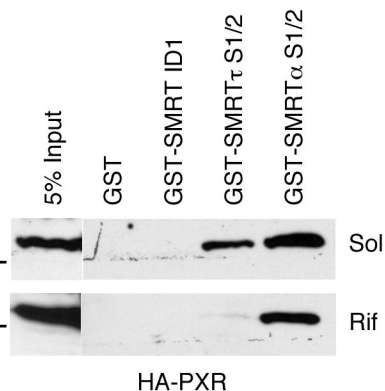
A



B



C



D

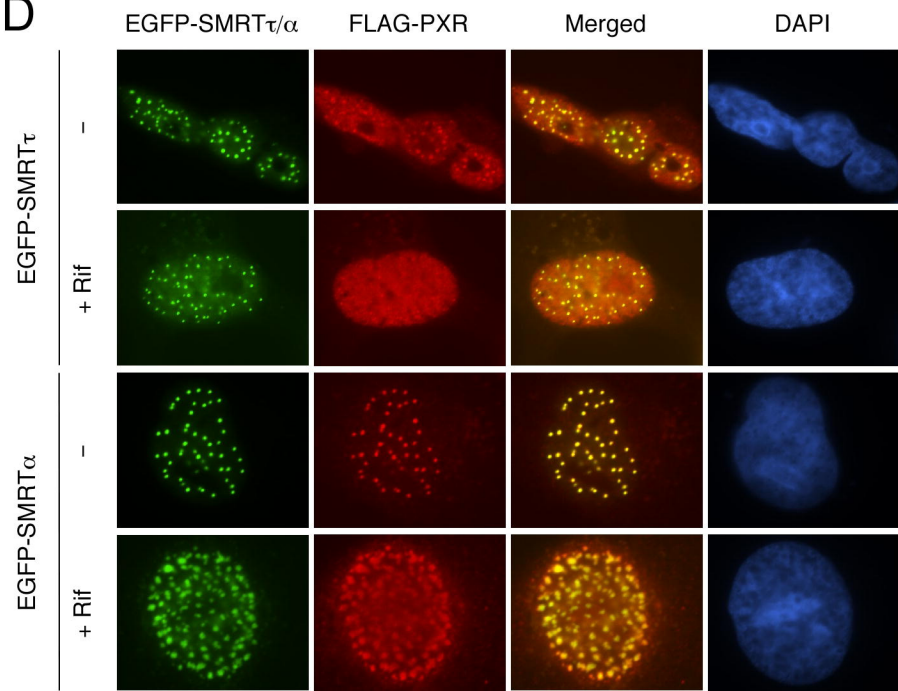
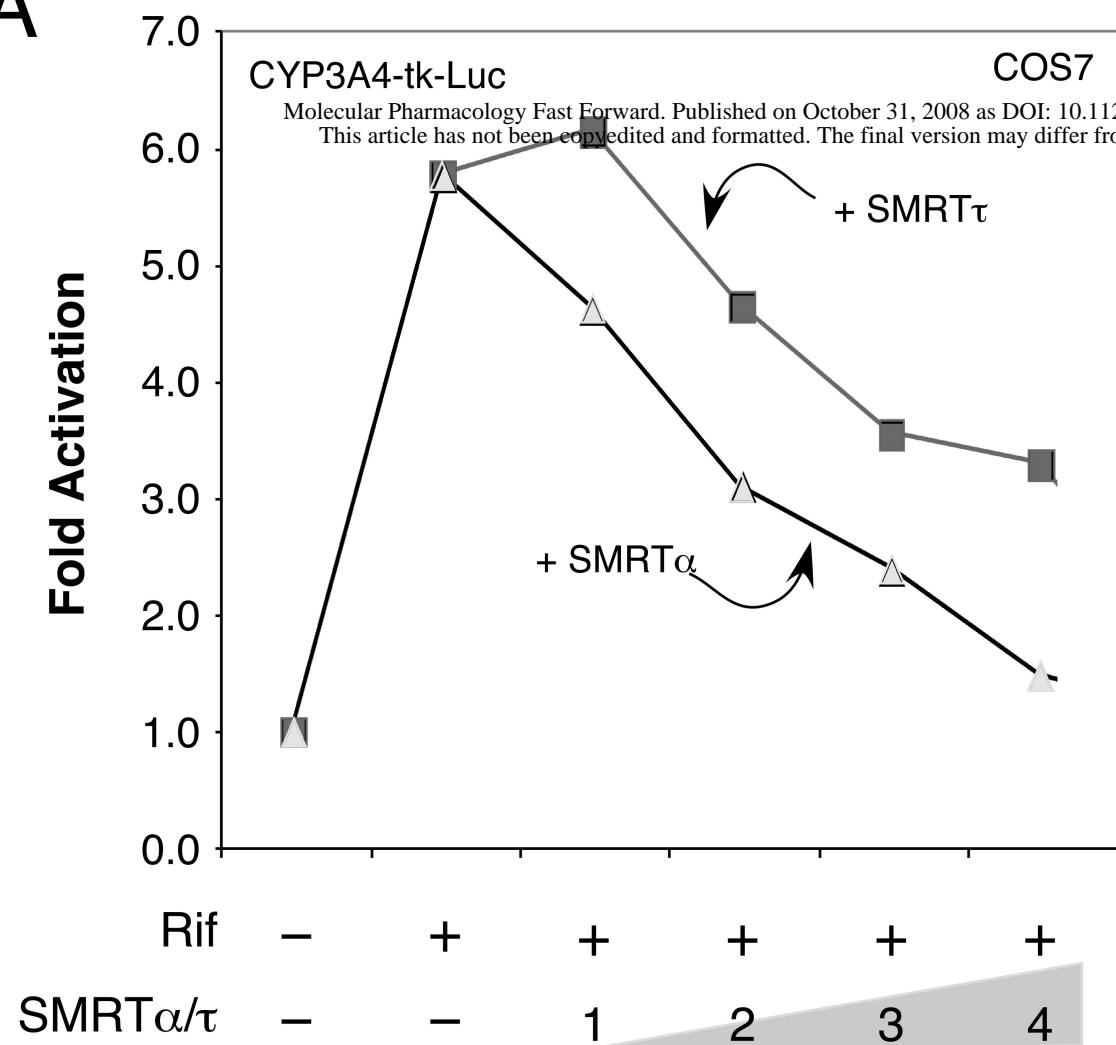
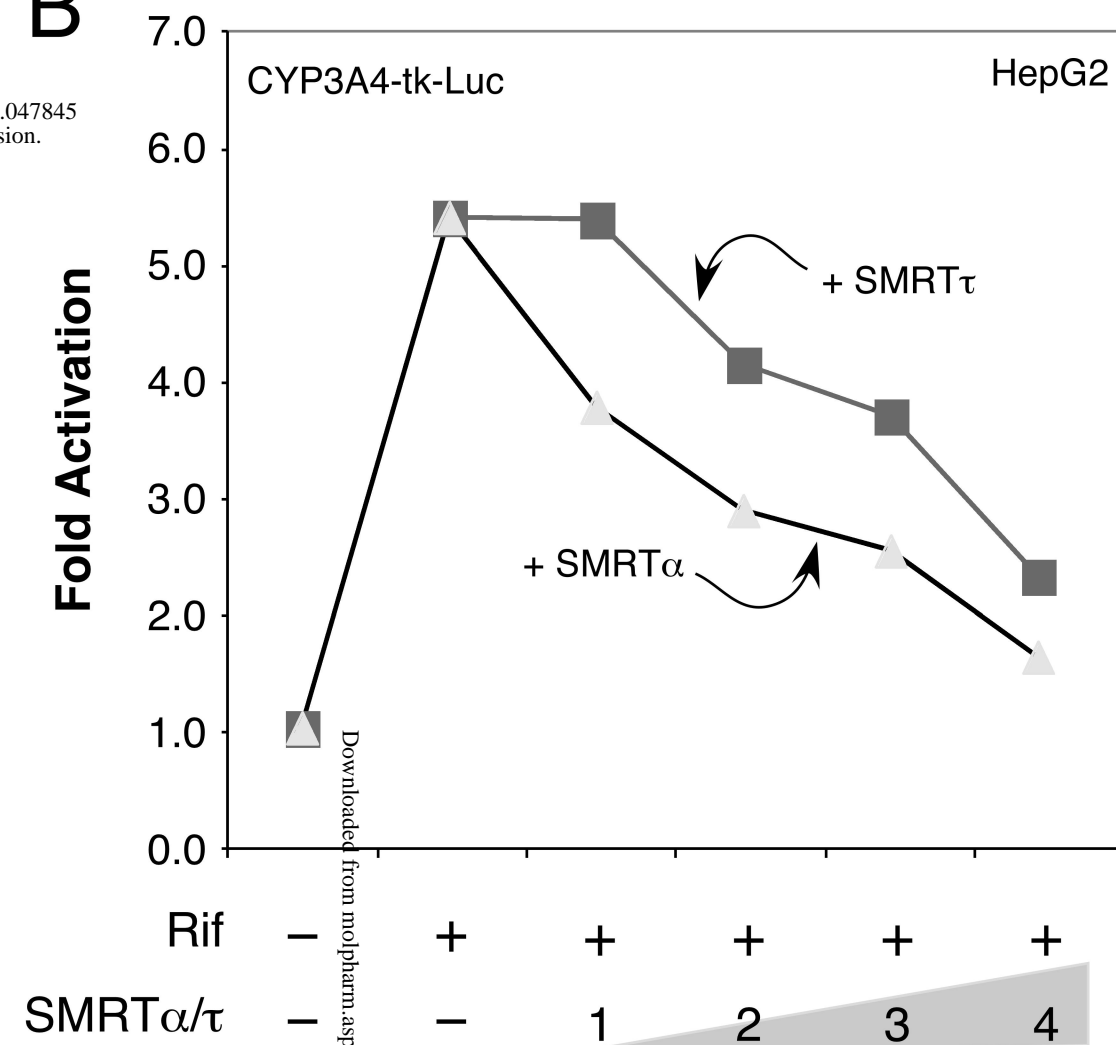


Figure 3

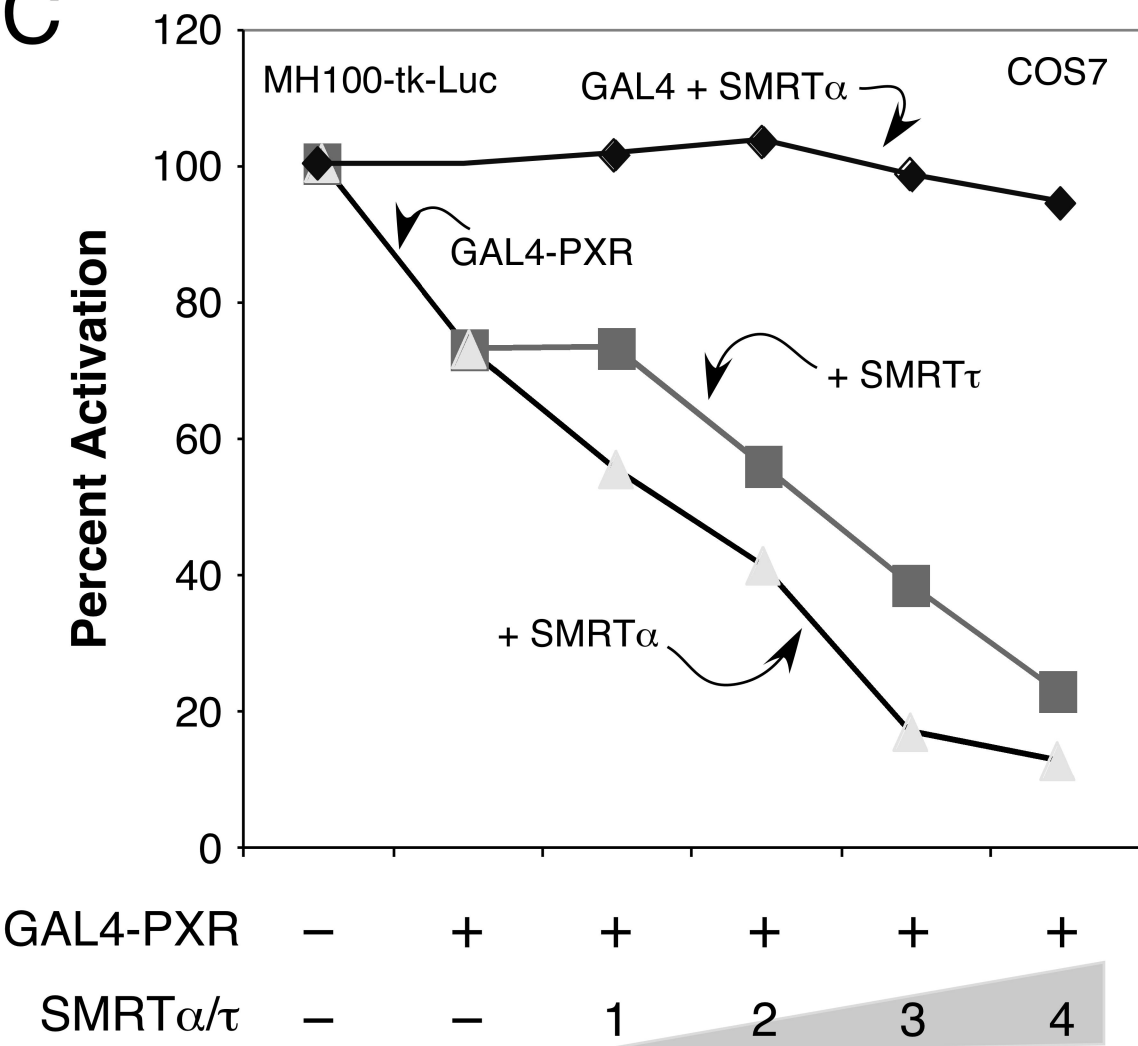
A



B



C



D

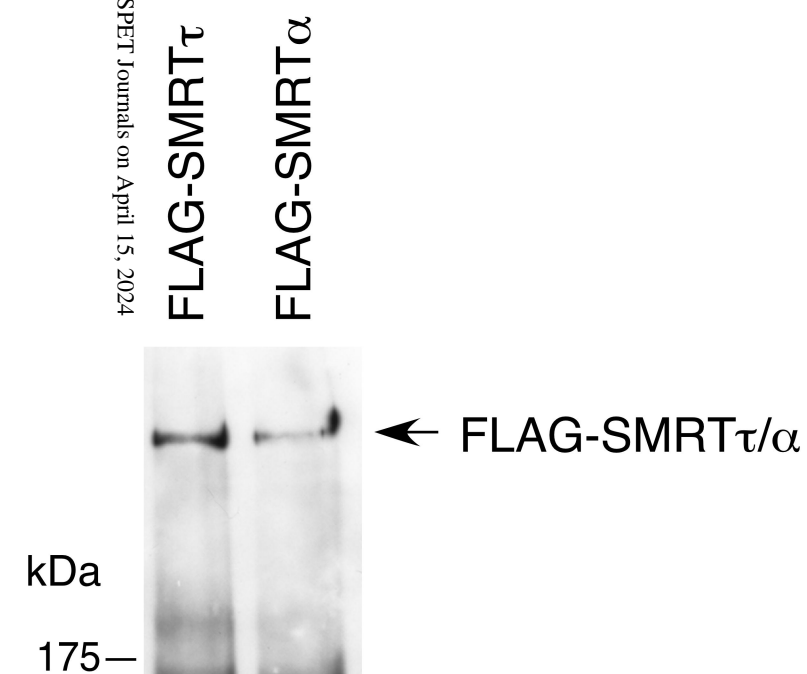
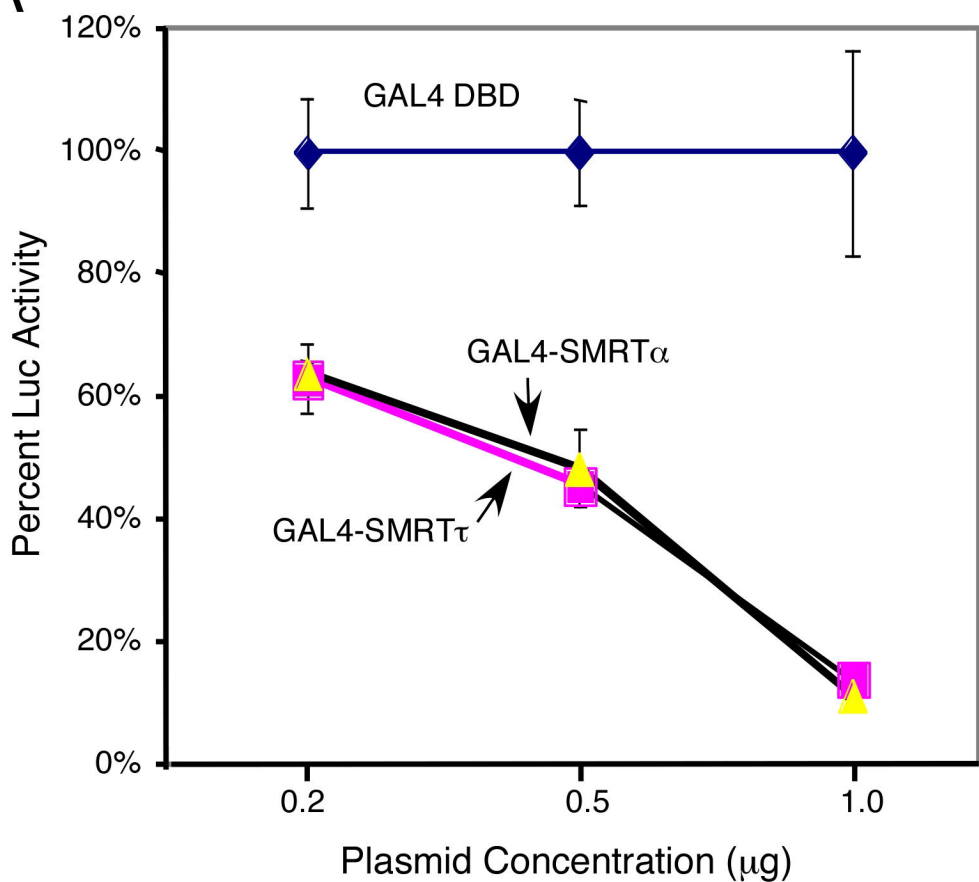


Figure 4

A



B

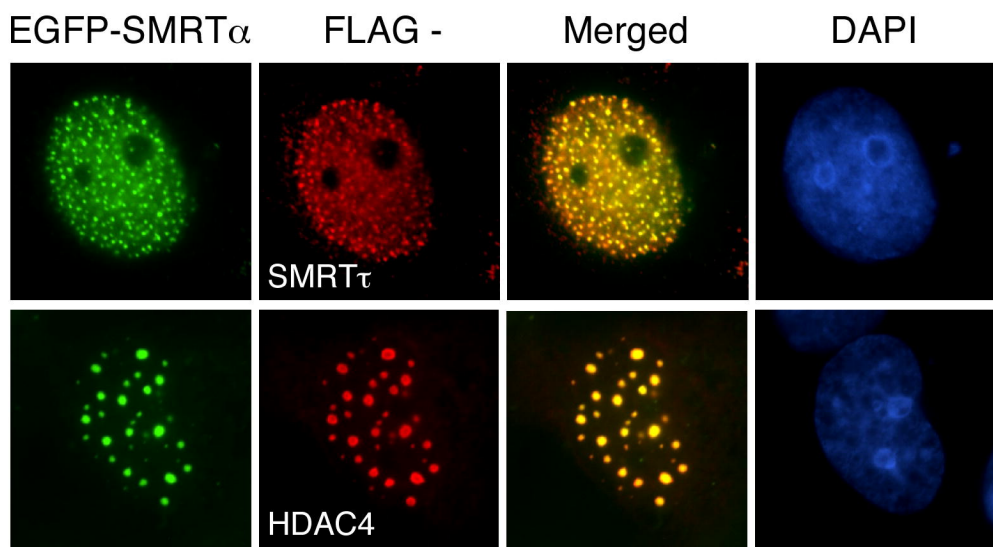
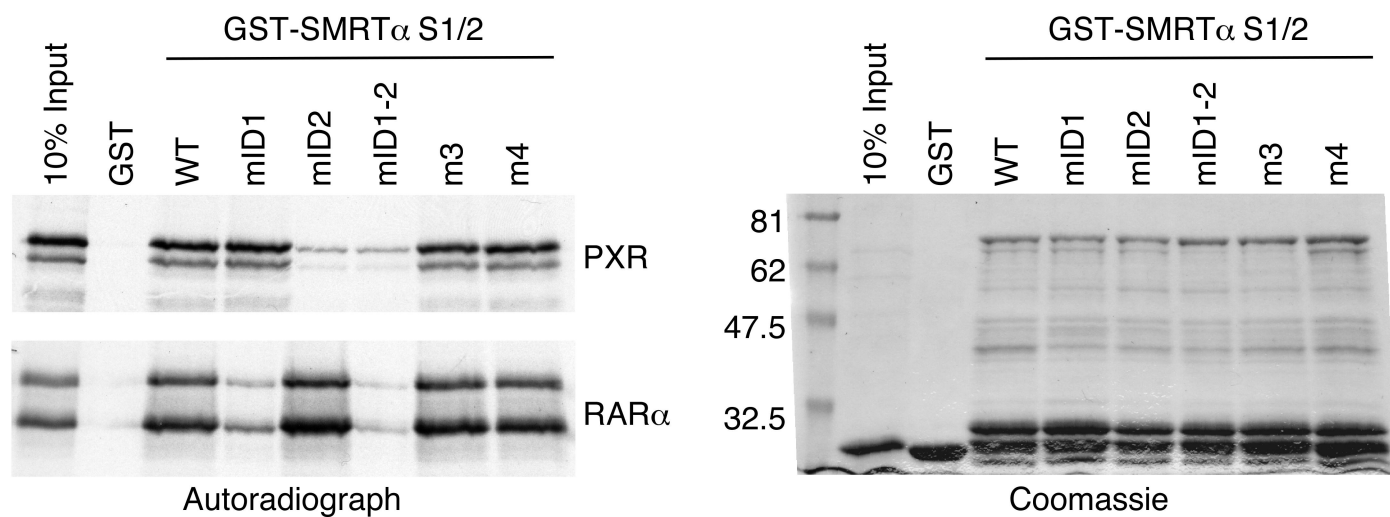


Figure 5

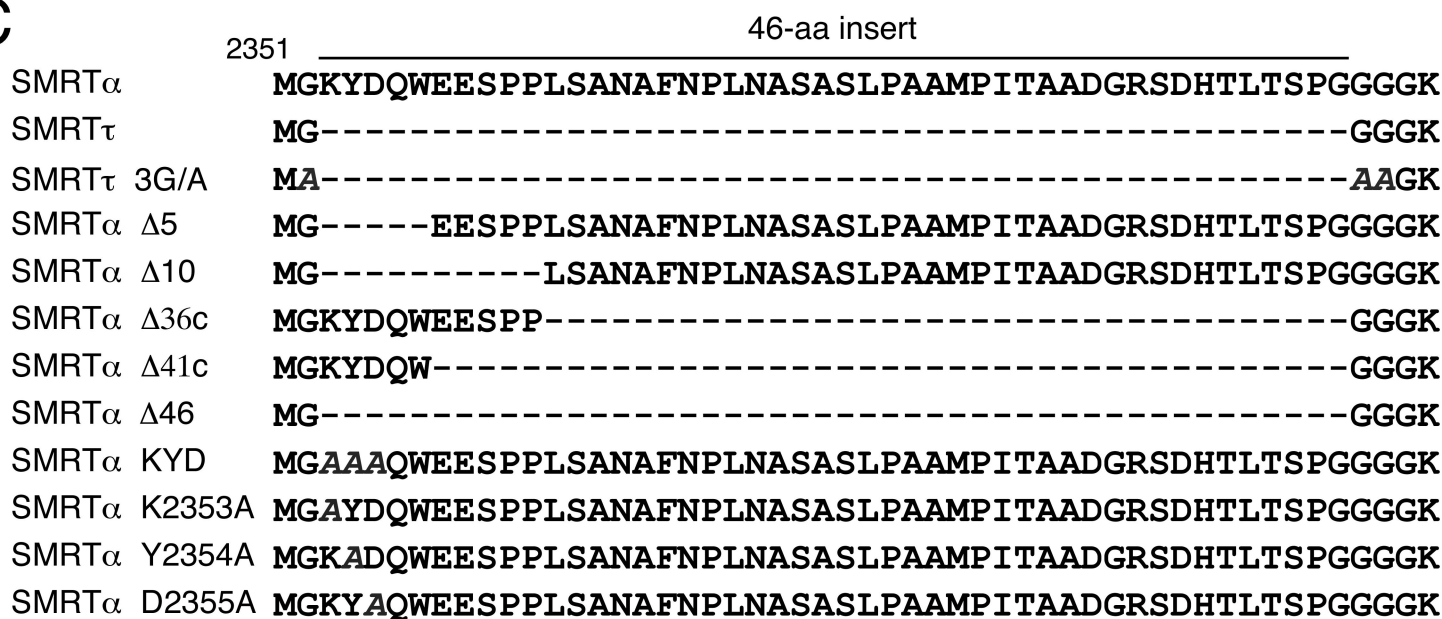
A



B



C



D

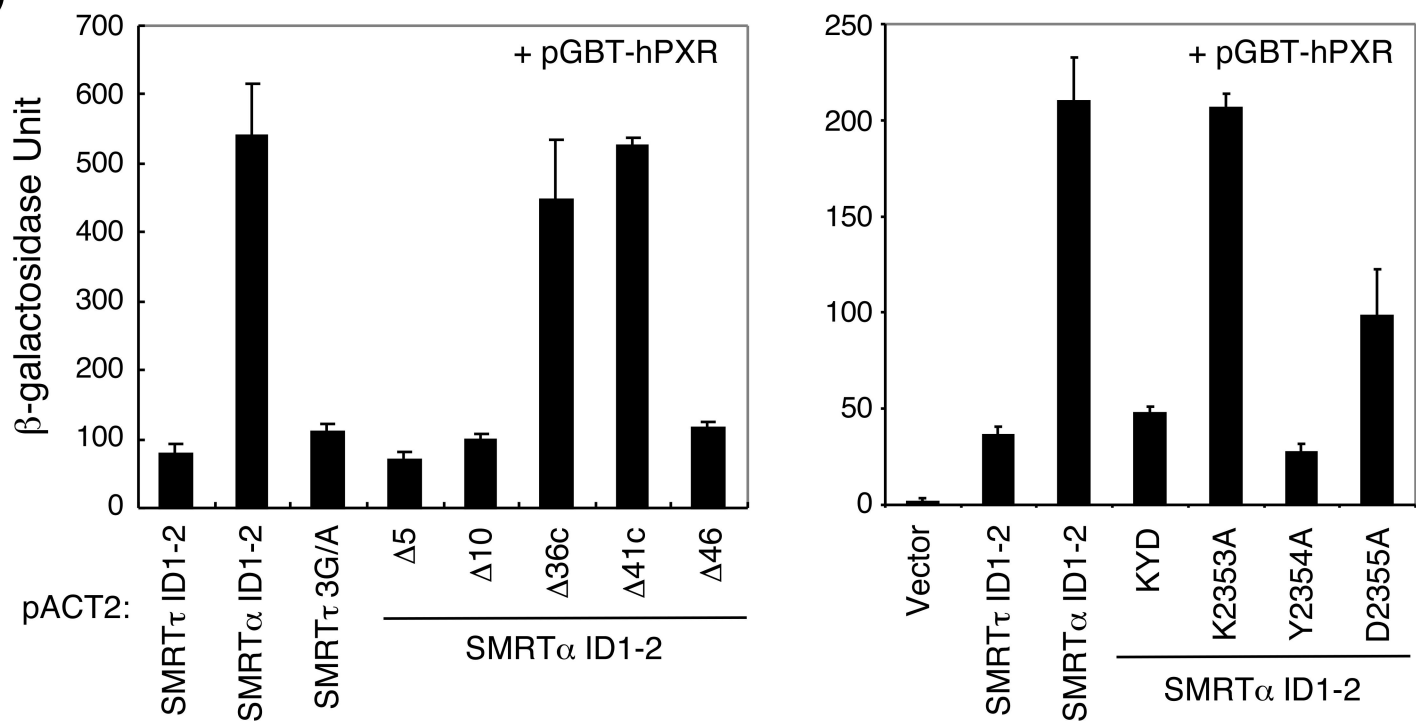
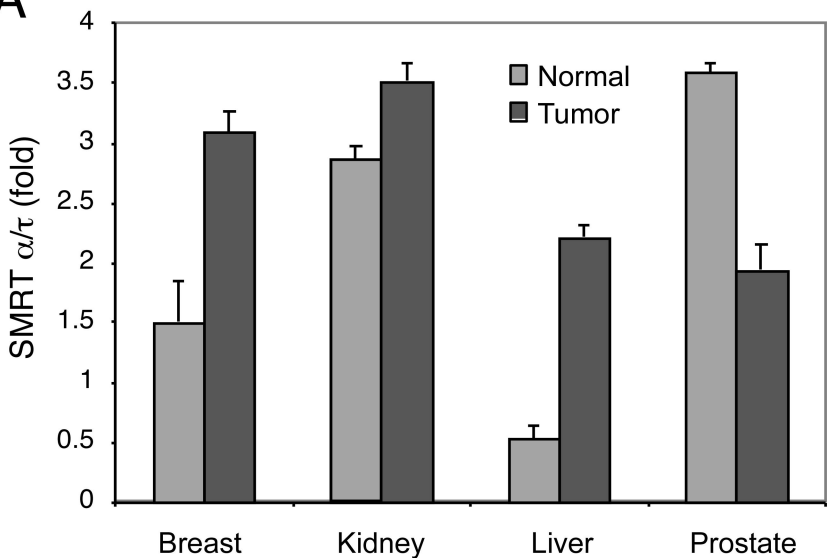
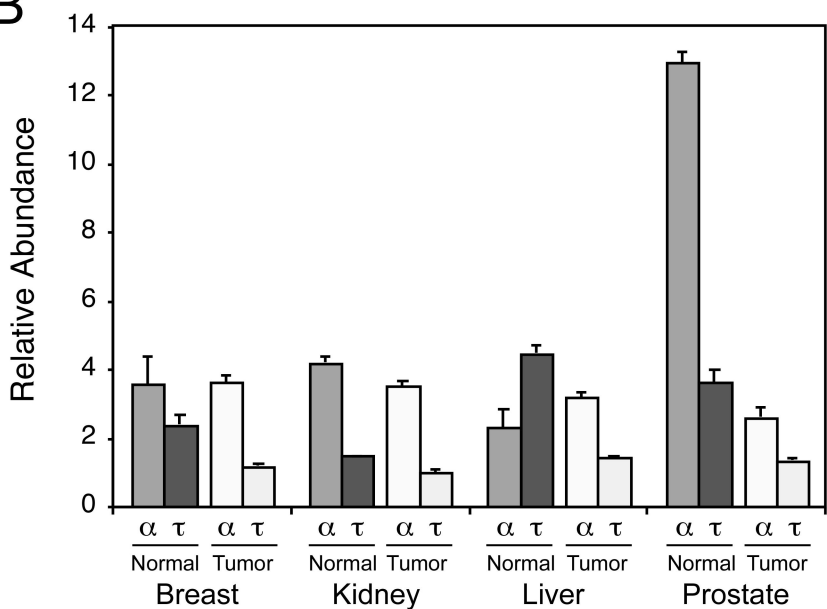


Figure 6

A



B



C

